PRAMANA — journal of physics

Vol. 79, No. 2
August 2012
pp. 299–310

Calibration-free laser-induced breakdown spectroscopy for quantitative elemental analysis of materials

V K UNNIKRISHNAN[1], K MRIDUL[1], R NAYAK[1], K ALTI[1], V B KARTHA[1], C SANTHOSH[1,*], G P GUPTA[2] and B M SURI[2]

[1]Centre for Atomic and Molecular Physics, Manipal University, Manipal 576 104, India
[2]Laser and Plasma Technology Division, Bhabha Atomic Research Centre, Mumbai 400 085, India
*Corresponding author. E-mail: santhosh.cls@manipal.edu

MS received 15 February 2011; revised 7 December 2011; accepted 1 March 2012

Abstract. The application of calibration-free laser-induced breakdown spectroscopy (CF-LIBS) for quantitative analysis of materials, illustrated by CF-LIBS applied to a brass sample of known composition, is presented in this paper. The LIBS plasma is produced by a 355 nm pulsed Nd:YAG laser with a pulse duration of 6 ns focussed onto a brass sample in air at atmospheric pressure. The time-resolved atomic and ionic emission lines of Cu and Zn from the LIBS spectra recorded by an Echelle spectrograph coupled with a gated intensified charge coupled detector are used for the plasma characterization and the quantitative analysis of the sample. The time delay where the plasma is optically thin and is also in local thermodynamic equilibrium (LTE), necessary for the elemental analysis of samples from the LIBS spectra, is deduced. An algorithm relating the experimentally measured spectral intensity values with the basic physics of the plasma is developed. Using the algorithm, the Zn and Cu concentrations in the brass sample are determined. The analytical results obtained from the CF-LIBS technique agree well with the certified values of the elements in the sample, with an accuracy error $<1\%$.

Keywords. Laser-induced plasma; plasma spectroscopy; quantitative elemental analysis.

PACS Nos 52.70.−m; 42.62.Fi; 52.50.Jm; 52.38.Mf

1. Introduction

Laser-induced breakdown spectroscopy (LIBS) [1], an emerging analytical technique, has many advantages: rapidity is high, can be used in multi-elemental analysis, only minimum sample is needed, sample destruction is minimum, low cost, can be used in a wide range of materials without any pre-processing and the experimental set-up is flexible. The technique is based on the generation of laser-induced plasma on a solid, liquid or gaseous sample by focussing a high-power pulsed laser beam with an irradiance

DOI: 10.1007/s12043-012-0298-1; ***e*Publication: 12 June 2012**

>100 MW/cm^2 onto the sample and the collection of light emitted from the plasma to be used to determine the elemental composition of the sample. In the recent past, it has been extended to a wide range of application areas, namely industrial material processing, analysis of archaeology and art works, determination of radioactive and hazardous materials, environmental monitoring, space exploration, military explosive detection and biomedical studies.

Quantitative LIBS analysis is conventionally performed using calibration-based method in which calibration curves of emission line intensity vs. elemental concentration using a few matrix-matched reference samples with known composition are first produced and then the composition of an unknown sample is found by comparing the analyte line signals with spectral intensities obtained from the calibration curves [2–7]. The applicability of this method is limited because a matrix with composition similar to the unknown sample is required which is, in many cases, not possible. As an alternative method, the calibration-free LIBS (CF-LIBS) method has been initially developed by Ciucci *et al* [8] for quantitative elemental analysis with LIBS spectra. In this method, the elemental composition of a sample is determined from the LIBS spectrum using computational methods in analysing the basic physics of the plasma process by estimating the plasma temperature and electron number density, assuming that the plasma composition represents exactly the composition of the sample, i.e. stoichiometric ablation, and the plasma is optically thin and is in local thermodynamic equilibrium (LTE). Since its inception, the CF-LIBS method has been used by several research groups across the world to analyse metallic alloys, such as Al-based [8,9], Fe-based [9], Cu-based [10–14] and Au-based [12,15] alloys as well as non-metallic samples, such as soil, rock and glass [12,14,16–18]. The advantage of this method is that the need for a matching matrix, a serious problem in the calibration-based LIBS, is overcome. A major drawback of this method is that one needs to detect at least one line of each element in the plasma with known atomic data. Gomba *et al* [19] have developed a CF-LIBS procedure different from that of Ciucci *et al* [8] to quantify the contents of the elements by estimating the plasma temperature, electron number density and relative number densities of the neutral and singly ionized ionic species in the LIBS plasma using the experimental spectral line intensity values in the time window where the plasma is optically thin and in LTE.

In the present work, we have applied the CF-LIBS technique, using the procedure developed by Gomba *et al* [19], to quantitatively analyse a brass sample of known composition (70% Cu and 30% Zn) placed in air at atmospheric pressure, in order to further evaluate the capabilities of the technique and establish the necessary conditions for accurate analysis by this procedure. For the quantification of elemental contents in the sample, we have developed an algorithm relating the experimentally measured spectral intensity values at a time delay where the plasma is optically thin and in LTE, with the basic physics parameters of the plasma. Using the algorithm we have determined the Zn and Cu concentrations in the brass sample. The analytical results obtained from CF-LIBS agree well with the certified values of the elements in the sample, with an accuracy error $<1\%$. Our studies show that by appropriate choice of experimental parameters and plasma conditions, accurate quantitative results can be obtained using the CF-LIBS technique. The results of our studies are presented and discussed below.

2. Experimental description

A schematic diagram of the experimental set-up used for LIBS experiments is depicted in figure 1. A pulsed Q-switched Nd:YAG laser (Spectra Physics PRO 230–10) working at the third harmonic wavelength of 355 nm with a 6 ns pulse duration and a 10 Hz repetition rate was focussed at right angles onto the sample surface, placed in air at atmospheric pressure using a bi-convex lens of focal length 20 cm. For an estimated value of the diameter of the focussed beam of $\sim$120 μm, the laser pulse irradiance on the sample was about 1.2×10^9 W/cm^2. The nanosecond, high irradiance, ultraviolet laser was used because it generates plasmas in atmospheric air with improved emission characteristics [20]. The laser irradiance, much larger than the threshold for plasma generation, ensures stoichiometric ablation even when there are large differences in the physical properties of the metal constituents [21]. The laser pulse induces plasma directly on the sample surface, thereby ablating a small crater and producing a plume of sampled material that moves away from the surface. The sample was mounted on a X-Y translation stage having a speed of 6 mm/s so that each laser pulse was incident on a fresh surface, thus maintaining the sample in the same conditions for different measurements. The spatially integrated plasma light emission was collected and imaged onto the spectrograph slit using an optical-fibre-based collection system. This collection system was positioned at a distance of about 20 cm from the plasma, making an angle 45° to the laser beam. An Echelle spectrograph-ICCD system (Andor Mechelle ME5000-DH734–18U-03PS150) was used to record the emission spectrum. The spectrograph with an Echelle grating covers 200–975 nm spectral range in a single shot with a good wavelength resolution (0.05 nm). The dispersed light from the spectrograph was collected by a thermoelectrically cooled ICCD camera which is sensitive in the whole UV–VIS–NIR spectral region converting the spectral signal into digital signal. A Hg–Ar lamp, which provides sharp lines from 200 to 1000 nm, was used for wavelength calibration of this system. Intensity calibration of the Echelle spectrograph-ICCD system was done using NIST-traceable deuterium–quartz–tungsten–halogen lamp (Model Ocean Optics DH 2000, USA).

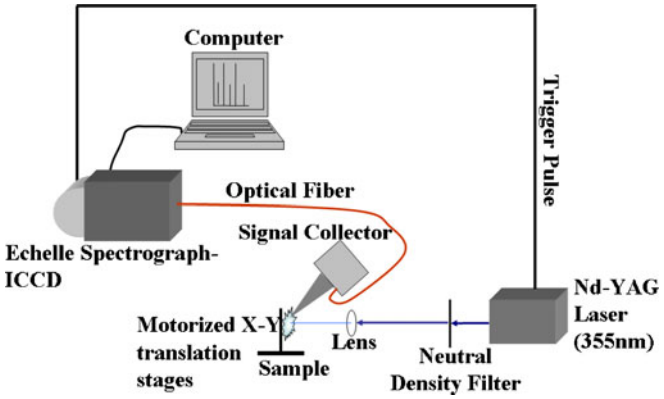

Figure 1. Experimental set-up for the LIBS system.

The detector was gated in synchronization with the laser pulse to get maximum signal-to-background (S/B) ratio. The detector gate width of 6 μs, which was found to be most advantageous in terms of the S/B ratio, was kept constant for all measurements. The continuum radiation from the LIBS plasma, which is intense at initial delay times of less than 300 ns, decreases to negligible values at later times. The detector gate delay was therefore varied in the 300–2000 ns time span for the optimization of experimental conditions. All LIBS spectra are derived from an integration of 120 laser pulses to minimize the effects of pulse-to-pulse variations from run to run.

3. Plasma characterization

For quantitative elemental analysis from the LIBS spectral line intensities, it is essential to characterize the time-evolving LIBS plasma in terms of its temperature and electron number density and find out the time window where the LIBS plasma is optically thin and in LTE. Based on plasma spectroscopy, the Boltzmann plot method yields the temperature T and the Saha–Boltzmann equation method yields the electron number density n_e of optically thin plasmas in LTE [22]. We have discussed these methods as well as the criterion for determining the plasma which is optically thin and in LTE, elsewhere [23] in characterizing laser-induced copper plasma. We briefly present below the relevant equations for characterizing the LIBS plasma using line intensities of the LIBS spectrum.

3.1 *Determination of plasma temperature T*

The integrated spectral line intensity of the k–i electronic transition of the species in charge state Z ($Z = 0$ for neutral atoms, $Z = 1$ for singly-ionized atoms, etc.) of element α in plasma which is optically thin and in LTE, is given as [22]

$$I^{\alpha}_{ki,Z} = F n^{\alpha}_{Z} \frac{g^{\alpha}_{k,Z} A^{\alpha}_{ki,Z}}{\lambda^{\alpha}_{ki,Z} P^{\alpha}_{Z}} \exp\left(-\frac{E^{\alpha}_{k,Z}}{k_{\mathrm{B}} T}\right), \tag{1}$$

where $F = hcL/4\pi$, L is the characteristic length of the plasma, h is the Planck constant, c is the speed of light, k_{B} is the Boltzmann constant, $E_{k,Z}$ and $g_{k,Z}$ are respectively the energy and degeneracy of the upper energy level k, $A_{ki,Z}$ is the transition line probability and $\lambda_{ki,Z}$ is the transition line wavelength of the k–i transition, P_Z is the partition function and n_Z is the number density of the species in ionization stage Z. By taking the natural logarithm, eq. (1) can be rewritten as

$$\ln\left(\frac{I^{\alpha}_{ki}\lambda^{\alpha}_{ki}}{g^{\alpha}_{k}A^{\alpha}_{ki}}\right) = -\frac{E^{\alpha}_{k}}{k_{\mathrm{B}}T} + \ln\left(\frac{Fn^{\alpha}}{P^{\alpha}}\right). \tag{2}$$

If the term on the left-hand side is plotted against E_k for two or more transition lines, the linear plot obtained is called the Boltzmann plot where the integral intensity of each spectral line is represented by a point in the Boltzmann plane. The slope of the Boltzmann plot yields the plasma temperature T.

3.2 *Determination of electron density n_e*

The electron density using atom and ion spectral lines emitted from the plasma is determined by employing the Saha–Boltzmann equation for the line intensities of the species in two consecutive charge states Z and $Z+1$ of a particular element as [19,22]

$$n_e = \frac{I'_Z}{I'_{Z+1}} 6.04 \times 10^{21} (T)^{3/2} \exp\left[\frac{\left(-E_{k,Z+1} + E_{k,Z} - \chi_Z\right)}{k_B T}\right] \text{cm}^{-3}, \tag{3}$$

where

$$I'_Z = \frac{I_Z \lambda_{ki,Z}}{g_{k,Z} A_{ki,Z}}$$

and χ_Z is the ionization energy of the species in the ionization state Z. The lowering of the ionization energy due to interactions in the plasma being negligibly small, is omitted in eq. (3).

3.3 *Determination of density ratio of the species of a particular element*

The Saha equation relating the concentrations in the two consecutive charge states Z and $Z+1$ of a particular element α is written as [19]

$$\frac{n_e n^\alpha_{Z+1}}{n^\alpha_Z} = 6.04 \times 10^{21} T_{\text{eV}}^{3/2} \frac{P^\alpha_{Z+1}}{P^\alpha_Z} \exp\left(-\frac{\chi^\alpha_Z}{T_{\text{eV}}}\right) \text{cm}^{-3}, \tag{4}$$

where T_{eV} is the plasma temperature in eV. This equation determines the value of the density ratio of the species in two consecutive charge states of a particular element, using experimentally determined values of T and n_e.

3.4 *Determination of density ratio of the species of different elements*

The density ratio of the species in different charge states of two elements is determined from the Saha–Boltzmann equation for the line intensities of the species in different charge states of two elements α and β as [19]

$$\frac{n^\alpha_Z}{n^\beta_{Z+1}} = \frac{I'_{\alpha,Z}}{I'_{\beta,Z+1}} \frac{P_{\alpha,Z}(T)}{P_{\beta,Z+1}(T)} \exp\left(-\frac{E_k^{\beta,Z+1} - E_k^{\alpha,Z}}{k_B T}\right). \tag{5}$$

3.5 *Criterion for plasma which is optically thin and in LTE*

The criterion to check whether the LIBS plasma is optically thin as well as in LTE, which is necessary for the quantitative composition analysis of the elements, using the LIBS spectra of a sample, is obtained from the intensity ratio of two lines of a particular element in the same charge state Z which is expressed as [23]

$$\frac{I_1}{I_2} = \left(\frac{\lambda_{nm,Z}}{\lambda_{ki,Z}}\right)\left(\frac{A_{ki,Z}}{A_{nm,Z}}\right)\left(\frac{g_{k,Z}}{g_{n,Z}}\right) \exp\left(-\frac{E_{k,Z} - E_{n,Z}}{k_B T}\right), \tag{6}$$

where I_1 is the line intensity from the k–i transition and I_2 is that from the n–m transition. If we consider two emission lines having the same upper level or as close as possible, the temperature effect of the Boltzmann factor on the reproducibility of the line intensity ratio is minimized and at the same time the consideration of the efficiency factor of the collecting system is avoided. Neglecting the exponential factor in that condition, one can find out the theoretical value of the intensity ratio of the two lines by using the atomic parameters of the transitions. By matching this theoretical intensity ratio with the measured values at different delay times, one finds out the time window where the plasma is optically thin and in LTE.

4. Quantitative elemental analysis

For quantitative elemental analysis using the CF-LIBS method, we have followed the CF-LIBS procedure developed by Gomba *et al* [19] where the concentrations of the elements are determined by matching theoretically obtained values of n_e and relative number densities of the neutral and singly ionized ionic species of a particular element as well as different elements in the plasma with those experimentally determined from eqs (3), (4) and (5) using the spectral line intensities in a time window where the LIBS plasma is optically thin and in LTE. The procedure used is as follows:

The total number density of element α is written as

$$n^{\alpha}_{\text{tot}} = n^{\alpha}_0 + n^{\alpha}_1 + n^{\alpha}_2 + \cdots n^{\alpha}_Z = n^{\alpha}_0 \left[1 + \sum_{Z=1}^{Z_N} \left(\frac{n^{\alpha}_Z}{n^{\alpha}_0} \right) \right], \tag{7}$$

where n^{α}_Z is the number density of the species of element α in charge state Z ($Z = 0$ for neutral atoms, $Z = 1$ for singly-ionized atoms, etc.). The element α contributes to the total n_e with n^{α}_e electrons from the atoms in different charge states, equal to the sum of all ionic state contributions, i.e.

$$n^{\alpha}_e = n^{\alpha}_1 + 2n^{\alpha}_2 + 3n^{\alpha}_3 + \cdots = \sum_{Z=1}^{Z_N} Z n^{\alpha}_Z. \tag{8}$$

Let us define the functions S^{α}_Z and R^{α}_Z as

$$S^{\alpha}_Z = \frac{n_e n^{\alpha}_{Z+1}}{n^{\alpha}_Z} = 6.04 \times 10^{21} T^{3/2}_{\text{eV}} \frac{P^{\alpha}_{Z+1}}{P^{\alpha}_Z} \exp\left(-\frac{\chi^{\alpha}_Z}{T_{\text{eV}}} \right) \text{cm}^{-3} \tag{9}$$

and

$$R^{\alpha}_Z = \frac{n^{\alpha}_Z}{n^{\alpha}_0}. \tag{10}$$

The function R^{α}_Z can be rewritten as

$$R^{\alpha}_Z = \frac{n^{\alpha}_Z}{n^{\alpha}_0} = \frac{n^{\alpha}_1}{n^{\alpha}_0} \frac{n^{\alpha}_2}{n^{\alpha}_1} \cdots \frac{n^{\alpha}_Z}{n^{\alpha}_{Z-1}} = \frac{S^{\alpha}_1}{n_e} \frac{S^{\alpha}_2}{n_e} \cdots \frac{S^{\alpha}_Z}{n_e} = \prod_{j=1}^{Z} \frac{S^{\alpha}_j}{(n_e)^Z}. \tag{11}$$

n^{α}_e, n^{α}_Z and $n^{\alpha}_Z / n^{\beta}_{Z+1}$ can be expressed in terms of R^{α}_Z as

$$n^{\alpha}_e = \frac{n^{\alpha}_{\text{tot}} \sum_{Z=1}^{Z_N} Z R^{\alpha}_Z}{1 + \sum_{Z=1}^{Z_N} R^{\alpha}_Z}, \tag{12}$$

$$n_Z^\alpha = \frac{n_{\text{tot}}^\alpha}{1 + \sum_{Z=1}^{Z_N} R_Z^\alpha} R_Z^\alpha, \tag{13}$$

$$\frac{n_Z^\alpha}{n_{Z+1}^\beta} = \frac{n_0^\alpha}{n_0^\beta} \frac{R_Z^\alpha}{R_{Z+1}^\beta}. \tag{14}$$

The total electron number density n_e of the plasma is obtained by summing up of electron contributions from all the elements:

$$n_e = \sum_{\alpha'=1}^{M} n_e^{\alpha'}, \tag{15}$$

where M is the total number of elements in the sample. Using T obtained from the Boltzmann plot and a proposed (initial) set of $n_{\text{tot}}^{\alpha'}$ of all the elements, n_e is calculated, incorporating electron contributions from all the elements, starting from its default value until convergence is reached. The converged value is taken as the theoretical value of n_e. Then, the values of $n_{Z+1}^\alpha/n_Z^\alpha$ and n_Z^α/n_{Z+1}^β are calculated. These calculations are carried out for a variable set of $n_{\text{tot}}^{\alpha'}$ of all the elements to find out an appropriate set of $n_{\text{tot}}^{\alpha'}$ of all the elements that results in the theoretical estimates of n_e, $n_{Z+1}^\alpha/n_Z^\alpha$ and n_Z^α/n_{Z+1}^β very close to the experimentally measured values. The relative concentration of element α is then obtained as

$$c^\alpha = \frac{n_{\text{tot}}^\alpha}{\sum_{\alpha'} n_{\text{tot}}^{\alpha'}}, \tag{16}$$

in terms of molar fractions or as

$$c^\alpha = \frac{n_{\text{tot}}^\alpha \mu_\alpha}{\sum_{\alpha'} n_{\text{tot}}^{\alpha'} \mu_{\alpha'}}, \tag{17}$$

in terms of mass abundance, where μ_α is the atomic weight of element α.

5. Results and discussion

In order to arrive at the proper time window for quantitative analysis, where the LIBS plasma is optically thin and in LTE, we have recorded the LIBS spectra of brass (70% Cu and 30% Zn) at five values of detector gate delay (300, 500, 700, 1000 and 2000 ns) relative to the laser pulse. A typical LIBS spectrum of brass at a time delay of 1000 ns is shown in figure 2. Three sets of such spectra are recorded at each of the five delays of interest. A mean value calculated from the spectra is used for the emission intensity of atomic and ionic lines. The variation of the experimental intensity ratio of two Cu I lines, 521.82 and 515.32 nm, having very close energies of their upper levels with the time delay is shown in table 1. The theoretical value of this intensity ratio is calculated from eq. (6) to be 1.8. Comparing the experimental data (within experimental errors) of the intensity ratio with the theoretical one, we have inferred the time delay of 1000 ns where the LIBS plasma is in LTE and optically thin. Hence, we have carried out further LIBS analysis at this time delay.

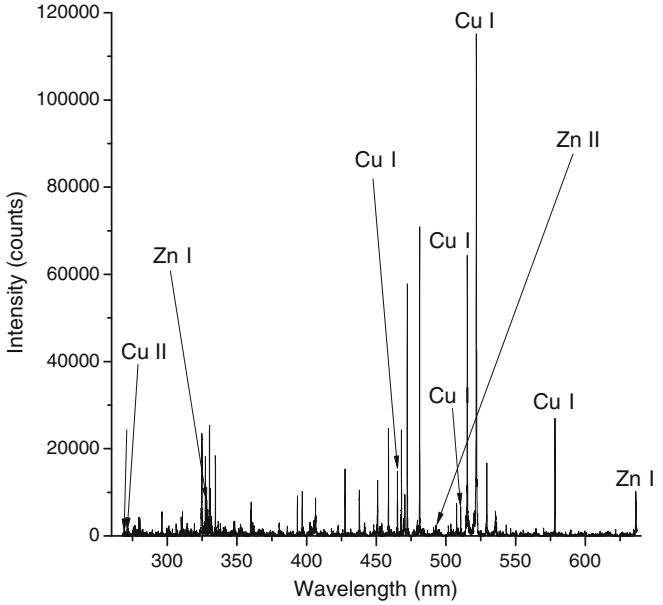

Figure 2. Typical LIBS spectrum of a brass sample at 1000 ns time delay.

The Boltzmann plot, generated using spectral line intensities of five Cu I transitions (465.11, 510.55, 515.32, 521.82 and 578.21 nm) at 1000 ns delay and their spectroscopic parameters as considered in our earlier work [23], is shown in figure 3. The plasma temperature inferred from the slope is 0.77 eV.

The electron number density is determined from eq. (3) using the measured intensity ratio of Cu I and Cu II lines as considered and discussed in our earlier work [23]. The value of n_e in the brass plasma at 1000 ns delay is obtained to be 1.10×10^{15} cm^{-3}.

We have determined the density ratio $n_{\mathrm{Cu\,II}}/n_{\mathrm{Cu\,I}}$ from eq. (4) using the measured values of T and n_e at the time delay of 1000 ns and the corresponding partition function from the NIST atomic database [24]. Its value is determined to be 65.7. The density ratio $n_{\mathrm{Zn\,I}}/n_{\mathrm{Cu\,II}}$ is determined from eq. (5) using the intensities of Zn I and Cu II lines at the time delay of 1000 ns and their spectroscopic parameters, taken from the NIST database

Table 1. Experimental intensity ratio of 521.82 nm Cu I line and 515.32 nm Cu I line as a function of time delay of the detector relative to the laser pulse.

Time delay (ns)	Intensity ratio
300	1.3
500	1.3
700	1.4
1000	1.6
2000	1.2

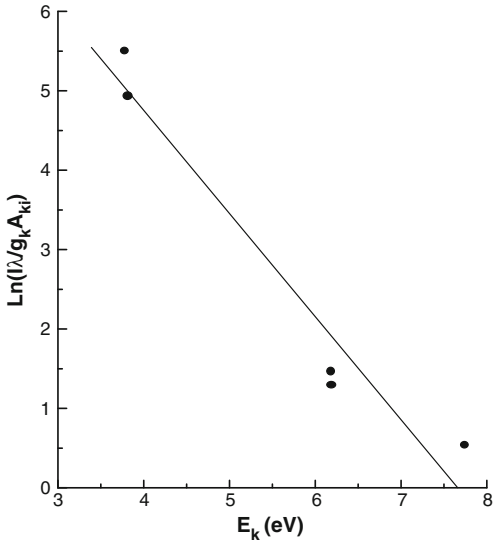

Figure 3. Boltzmann plot made using five Cu I lines, considering the intensities at a time delay of 1000 ns. The slope gives the temperature equal to 0.77 eV.

[24]. The atomic and ionic lines chosen in the present work are well resolved and free from spectral interference. We have considered three intensity ratios, 636.23 nm Zn I and 268.93 nm Cu II, 636.23 nm Zn I and 271.35 nm Cu II and 328.23 nm Zn I and 271.35 nm Cu II and obtained the values of $n_{\mathrm{Zn\,I}}/n_{\mathrm{Cu\,II}}$. The average value of $n_{\mathrm{Zn\,I}}/n_{\mathrm{Cu\,II}}$ as the arithmetic mean of the three values is determined to be equal to 1.163×10^{-2}. These experimental results are shown in table 2.

For the quantification of elemental contents in the sample, we have developed an algorithm based on the procedure discussed in §4. A schematic diagram of the CF-LIBS algorithm used in this work is shown in figure 4. We have varied the values of $n_{\mathrm{tot}}^{\mathrm{Cu}}$ and $n_{\mathrm{tot}}^{\mathrm{Zn}}$ in the range 10^{13}–10^{15} cm^{-3} in the algorithm and calculated the values of n_{e}, $n_{\mathrm{Zn\,I}}/n_{\mathrm{Cu\,II}}$ and $n_{\mathrm{Cu\,II}}/n_{\mathrm{Cu\,I}}$ in the LIBS plasma as the theoretical results, which match well with the experimental results when $n_{\mathrm{tot}}^{\mathrm{Zn}} = 3.3 \times 10^{14}\mathrm{cm}^{-3}$ and $n_{\mathrm{tot}}^{\mathrm{Cu}} = 8.0 \times 10^{14}\mathrm{cm}^{-3}$ are considered. Using these density values we have determined the fractional molar concentrations of Zn and Cu in the brass sample. The values of Zn and Cu concentrations in the brass sample obtained from the CF-LIBS analysis along with their certified values are shown in

Table 2. Values of T, n_{e}, $n_{\mathrm{Zn\,I}}/n_{\mathrm{Cu\,II}}$ and $n_{\mathrm{Cu\,II}}/n_{\mathrm{Cu\,I}}$ in the LIBS plasma determined from the LIBS spectral line intensities as experimental results.

T (eV)	n_{e} (cm^{-3})	$n_{\mathrm{Zn\,I}}/n_{\mathrm{Cu\,II}}$	$n_{\mathrm{Cu\,II}}/n_{\mathrm{Cu\,I}}$
0.77	1.10×10^{15}	1.163×10^{-2}	65.7

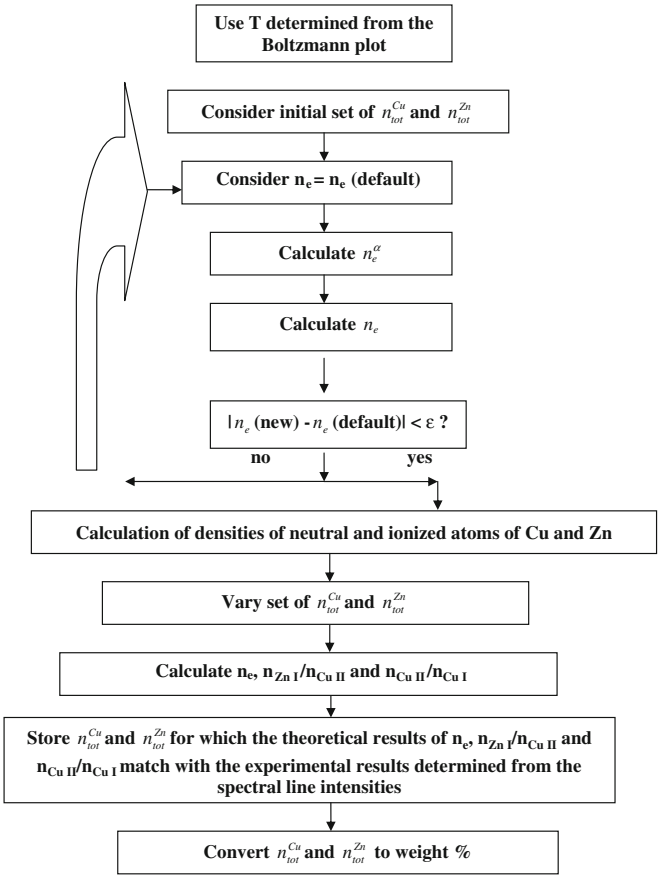

Figure 4. Schematic diagram of the CF-LIBS algorithm used in this work.

table 3. The accuracy errors of the LIBS analytical results are also given in the table. It is noted from the table that the analytical results obtained from CF-LIBS agree very well with the certified values of the elements in the sample, with an accuracy error $<1\%$.

The advantages of LIBS over conventional spectrochemical analytical methods depend on the possibility of forming an emission source which is fully representative of the sample (total evaporation), even through remote operation. This allows LIBS to be used in

Table 3. Values of Zn and Cu concentrations obtained from the CF-LIBS analysis along with their certified values and accuracy errors of the LIBS analytical results.

Zn concentration (wt %)		Cu concentration (wt %)		Accuracy error (%)	
CF-LIBS	Certified	CF-LIBS	Certified	Zn	Cu
29.794	30	70.206	70	0.7	0.3

situations where no calibration standards or even internal standards for normalization of data can be considered, for example, space applications, remote analysis of hostile environments like areas of nuclear accidents, terrorist operations, conditions of hostilities, one-of-a-kind industrial installations etc., where no *a priori* knowledge of the possible composition of the sample is available. The present work shows that in such situations, accurate quantitative analysis of materials with totally unknown composition, could be achieved by LIBS, provided standard spectroscopic data on spectral lines of the elements to be analysed are available.

In conventional methods, one normally carries out many sample pre-processing steps and even control the emission/absorption. It is therefore necessary to standardize the method using a matrix similar to the sample, and prepare standards under the same conditions, with the addition of known amounts of analyte. Obviously, this is not possible for the analytical applications envisaged under the present work. Including different 'standards' is not going to show anything different since Standard X is as good as Standard Y and each 'standard' will be analysed by plasma conditions of that 'standard'. Since absolutely no assumptions are involved in the actual calculations, and the entire sample is brought in the emission system, the results are entirely independent of the material composition. Unlike conventional laboratory analytical techniques, one does not have to verify the applicability of the method by using multiple standards and preparing a calibration curve. If the matching of the LIBS-determined value with the certified value occurs in one sample, it will also occur in other samples as shown by Gomba *et al* [19].

6. Conclusions

We have successfully carried out the quantitative analysis of a certified brass sample using the CF-LIBS technique. From the time-resolved spectral intensities of Cu I lines from the LIBS plasma, the appropriate time delay, where LTE and optically thin plasma conditions are satisfied, is determined. The LIBS plasma formed on the surface of brass at this time delay is characterized by determining the plasma temperature and electron number density. We have also determined the density ratio of the species in different charge states of the two elements (Zn and Cu) in the sample using the line intensities of the species in different charge states of the two elements. An algorithm relating the experimentally measured spectral intensity with the basic physics of the plasma is developed for the quantitative analysis of the materials. The present algorithm is applied to a brass sample and the Zn and Cu concentrations in the sample are determined. The elemental concentrations obtained from the CF-LIBS technique are in very good agreement with the certified values. It is concluded that accurate quantitative analysis can be achieved using the CF-LIBS technique, by choosing the appropriate plasma conditions.

Acknowledgements

The authors are thankful to BRNS, DAE, Govt. of India for the financial support provided through a LIBS project (Project No. 2007/34/14-BRNS).

References

[1] D A Cremers and L J Radziemski, *Handbook of laser-induced breakdown spectroscopy* (John Wiley & Sons Ltd, West Sussex, 2006)
[2] C Aragon, J A Aguilera and F Penalba, *Appl. Spectrosc.* **53**, 1259 (1999)
[3] I Bassiotis, A Diamantopoulou, A Giannoudakos, F R Kalantzopoulou and M Kompitsas, *Spectrochim. Acta* **B56**, 671 (2001)
[4] J D Winefordner, I B Gornushkin, T Correll, E Gibb, B W Smith and N Omenetto, *J. Anal.At. Spectrom.* **19**, 1061 (2004)
[5] B Salle, D A Cremers, S Maurice and R C Wiens, *Spectrochim. Acta* **B60**, 479 (2005)
[6] G Cristoforetti, S Legnaioli, V Palledchi, A Salvetti, E Tognoni, P A Benedetti, F Brioschi and F Ferrario, *J. Anal. At. Spectrom.* **21**, 697 (2006)
[7] G P Gupta, B M Suri, A Verma, M Sunderaraman, V K Unnikrishnan, K Alti, V B Kartha and C Santhosh, *J. Alloys Compd.* **509**, 3740 (2011)
[8] A Ciucci, V Palleschi, S Rastelli, A Salvetti and E Tognoni, *Appl. Spectrosc.* **53**, 960 (1999)
[9] E Tognoni, G Cristoforetti, S Legnaioli, V Palleschi, A Salvetti, M Mueller, U Panne and I Gornushkin, *Spectrochim. Acta* **B62**, 1287 (2007)
[10] F Colao, R Fantoni, V Lazic, I Caneve, A Giardini and V Spizzichino, *J. Anal. At. Spectrom.* **19**, 502 (2004)
[11] I Fornarini, F Colao, R Fantoni, V Lazic and V Spizzichino, *Spectrochim. Acta* **B60**, 1186 (2005)
[12] V S Burakov and S N Raikov, *Spectrochim. Acta* **B62**, 217 (2007)
[13] J A Aguilera, C Aragon, G Cristoforetti and E Tognoni, *Spectrochim. Acta* **B64**, 685 (2009)
[14] K K Herrera, E Tognoni, N Omenetto, B W Smith and J D Winefordner, *J. Anal. At. Spectrom.* **24**, 413 (2009)
[15] M V Belkov, V S Burakov, V V Kiris, N M Kozhukh and S N Raikov, *J. Appl. Spectrosc.* **72**, 376 (2005)
[16] F Colao, R Fantoni, V Lazic, A Paolini, F Fabbri, G G Ori, L Marinangeli and A Baliva, *Planet. Space Sci.* **52**, 117 (2004)
[17] B Salle, J I Lacour, P Mauchien, P Fichet, S Maurice and G Manhes, *Spectrochim. Acta* **B61**, 301 (2006)
[18] A De Giacomo, M Dell'Aglio, O De Pascale, S Longo and M Capitelli, *Spectrochim. Acta* **B62**, 1606 (2007)
[19] J M Gomba, C D'Angelo, D Bertuccelli and G Bertuccelli, *Spectrochim. Acta* **B56**, 695 (2001)
[20] K Kagawa, K Kawai, M Tani and T Kobayashi, *Appl. Spectrosc.* **48**, 198 (1994)
[21] X L Mao, A C Ciocan, O V Borisov and R E Russo, *Appl. Surf. Sci.* **127–129**, 262 (1998)
[22] H R Griem, *Principles of plasma spectroscopy* (Cambridge University Press, Cambridge, 1997)
[23] V K Unnikrishnan, K Alti, V B Kartha, C Santhosh, G P Gupta and B M Suri, *Pramana – J. Phys.* **74**, 983 (2010)
[24] NIST Atomic Spectra Database, http://physics.nist.gov.